Published in final edited form as:
Biomaterials. 2014 June ; 35(17): 4729–4738. doi:10.1016/j.biomaterials.2014.02.002.

Aqueous cationic, anionic and non-ionic multi-walled carbon nanotubes, functionalised with minimal framework damage, for biomedical application

Shu Chen[a,‡], **Sheng Hu**[b,‡], **Elizabeth F. Smith**[c], **Pakatip Ruenraroengsak**[a], **Andrew J. Thorley**[c], **Robert Menzel**[b], **Angela E. Goode**[a], **Mary P. Ryan**[a], **Teresa D. Tetley**[c], **Alexandra E. Porter**[a], and **Milo S. P. Shaffer**[b,*,†]

[a]Department of Materials and London Centre for Nanotechnology, Imperial College London, Exhibition Road, London SW7 2AZ, UK

[b]Department of Chemistry and London Centre for Nanotechnology, Imperial College London, Exhibition Road, London SW7 2AZ, UK

[c]National Heart and Lung Institute, Imperial College London, Dovehouse Street, London SW3 6LY, UK

Abstract

The use of a thermochemical grafting approach provides a versatile means to functionalise as-synthesised, bulk multi-walled carbon nanotubes (MWNTs) without altering their inherent structure. The associated retention of properties is desirable for a wide range of commercial applications, including for drug delivery and medical purposes; it is also pertinent to studies of intrinsic toxicology. A systematic series of water-compatible MWNTs, with diameter around 12 nm have been prepared, to provide structurally-equivalent samples predominantly stabilised by anionic, cationic, or non-ionic groups. The surface charge of MWNTs was controlled by varying the grafting reagents and subsequent post-functionalisation modifications. The degree of grafting was established by thermal analysis (TGA). High resolution transmission electron microscope (HRTEM) and Raman measurements confirmed that the structural framework of the MWNTs was unaffected by the thermochemical treatment, in contrast to a conventional acid-oxidised control which was severely damaged. The effectiveness of the surface modification was demonstrated by significantly improved solubility and stability in both water and cell culture medium, and further quantified by zeta-potential analysis. The grafted MWNTs exhibited relatively low bioreactivity on human immortal alveolar epithelial type 1-like cells (TT1) following 24h exposure as demonstrated by 3-(4,5-dimethylthiazol-2-yl)-5-(3-carboxymethoxyphenyl)-2-(4-sulfophenyl)-2H-

[†]Electronic supplementary information (ESI) available: Grafting ratio calculation, details of Raman spectroscopy of carbon nanotubes and TEM cell uptake images of AR- and P(MAA)-MWNTs

[*]Corresponding author. Department of Chemistry and London Centre for Nanotechnology, Imperial College London, Exhibition Road, London SW7 2AZ, UK. m.shaffer@imperial.ac.uk (M.S. P. Shaffer).
[‡]These authors contributed equally to this work

tetrazolium (MTS) and lactate dehydrogenase release (LDH) assays. The exposure of TT1 cells to MWNTs suppressed the release of the inflammatory mediators, interleukin 6 (IL-6) and interleukin 8 (IL-8). TEM cell uptake studies indicated efficient cellular entry of MWNTs into TT1 cells, via a range of mechanisms. Cationic MWNTs showed a more substantial interaction with TT1 cell membranes than anionic MWNTs, demonstrating a surface charge effect on cell uptake.

Keywords

Multiwalled carbon nanotubes; Thermal chemical functionalisation; Integrity structure; Surface charge; Cytotoxicity; Cell uptake

1 Introduction

The biological interactions of carbon nanotubes (CNTs) are important for fundamental scientific studies [1, 2], biomedical applications such as photothermal therapy [3, 4], drug delivery [5, 6] and bioimaging [7, 8], and in order to understand their potential toxicities [5, 9, 10]. The poor solubility and lack of control over the physicochemical properties of CNTs have created significant obstacles to understanding their interactions with cells. Delivery of individualised CNTs either *in vitro* in cell medium or *in vivo* is rare, particularly for toxicology studies, in which agglomerated or even non-aqueous dispersions are commonly used. Surfactants, such as Triton X-100 [5, 6, 11] and sodium dodecyl sulfate (SDS) [7, 8, 12], can be used to stabilise aqueous dispersions but use is limited by surfactant toxicity which can cause confounding effects [9, 10, 13] and do not relate to many real life situations. In addition, surfactant dispersions are meta-stable, with a surface chemistry that evolves over time, and are generally unsuitable for *in vivo* use [14]. Where modified, water-stabilised CNTs have been used, the chemistry or dispersion processes introduce damage or dimensional change [15, 16], limiting controlled comparisons. Improved protocols are needed to produce water compatible CNTs with well-defined dimensions whilst minimising changes to their intrinsic properties. Furthermore, surface modification of MWNTs can provide a product with enhanced and desirable properties for medicinal and other purposes. In addition, reasonably large quantities are required for consistent sets of *in vivo* and *in vitro* experiments, as well as a wide range of other CNT applications [17, 18] in which aqueous processing would be advantageous.

One of the most common approaches for preparing water dispersions of CNTs relies on oxidation using strong acids, particularly mixtures of HNO_3 and H_2SO_4 [19, 20]. This covalent functionalisation method produces good aqueous dispersions [20], and provides a high degree of functionalisation with -COOH groups suitable for further modification [21, 22]. However, CNT walls are inevitably etched, the length is significantly reduced [23, 24], and the sample is contaminated with oxidation reaction debris, also known as carboxylated carbonaceous fragments (CCFs), which are difficult to completely remove [25–27], and may contribute to cytotoxic effects [28, 29]. Although the cytotoxicity of the oxidation debris is not yet fully understood, it has been shown that these CCFs can significantly alter the physicochemical properties and biological interactions of the acid-oxidised CNTs [25, 26,

30, 31]. Further, the oxidation reaction also introduces a wide range of different, oxygen-containing functional groups, obscuring the nature of the underlying CNTs and generating an ill-defined generally acidic surface. Derivitising these surface functional groups (or, in some cases, unremoved debris) to form other chemical functionalities does not counter the remaining fundamental drawbacks [32]. Other chemical methods have also been explored [33, 34], but a versatile, scalable method for varying surface character independently of other characteristics is still needed. The recent development of a solvent-free thermochemical grafting approach offers advantages in the preparation of large quantities of clean, functionalised MWNTs with minimal framework damage [35]. The approach takes advantage of existing defective groups on the MWNT surface, remaining from the synthesis process, which decompose at high temperatures and generate free radicals, allowing covalent grafting of a range of monomers [35]. The intrinsic framework of the MWNTs is preserved and there is no production of debris or use of corrosive solutions. The approach is readily scalable as it is compatible with common chemical vapor deposition (CVD) capital infrastructure and can be operated to avoid time-consuming filtration steps. Here, this protocol was developed to produce water-compatible MWNTs with cationic, anionic or neutral character for biological studies. The vast majority of nanotubes produced commercially are multi-walled structures prepared by CVD; these materials are produced in significant quantities, by different companies, but with similar characteristics [36], and are most relevant to near term application and occupational hazards.

The effects of MWNTs on lung cells are particularly relevant to discovering possible nanotoxicological pathways, since inhalation is considered to be one of the greatest exposure risks [37, 38]. Similar to other thin materials, regardless of length, MWNTs with diameters smaller than 1 μm are respirable and may be able to travel deeply into the lung alveolar region, where the thin gas–blood barrier (in some places < 0.5 μm deep) is located to allow gas exchange [39, 40]. Alveolar macrophages are the first line of defence against particulate material which deposit in the alveoli. Particles are taken up into macrophages through phagocytosis, and subsequently cleared out of the lung via the mucociliary escalator and lymphatic system. Particles that are not phagocytosed by macrophages will interact with the alveolar epithelium [40, 41], which comprises a monolayer of alveolar type I (AT1) and alveolar type II (AT2) epithelial cells [42]. AT1 cells, which cover >95% of the alveolar surface area, are large squamous cells that facilitate gas exchange [43]. There is some concern that the interaction of high aspect ratio particles with alveolar epithelial cells could induce similar pathologies to those observed with high aspect ratio amphibole asbestos, including epithelial cell necrosis or apoptosis, release of pro-inflammatory cytokines, which could compromise the integrity of the epithelium, and increase the chance of particle translocation across the gas-blood barrier to the interstitium and systemic circulation [44]. This paper describes the generation and properties of a panel of surface functionalized MWNTs with anionic, cationic or non-ionic groups and high water solubility, relevant to a wide range of applications. Here, their bioreactivity with the human lung epithelium is studied *in vitro*. The effects on TT1 cell viability and mediator release have been assessed and the extent of uptake studied by TEM.

2 Materials and Methods

2.1 Carbon nanotubes and chemicals

MWNTs (diameter 12.1 nm, s.d. 3.7 nm), synthesised by CVD, were obtained from Arkema SA (Lacq-Mourenx, France). Methyl methacrylate (MMA, > 98.5%), 4-vinyl pyridine (4-VP, 95%), poly(ethylene glycol) methacrylate (PEGMA, average M_n = 530), 1-iodododecane (IDD, 98%), iodomethane (IMe, ≥ 99%), and lithium hydroxide (LiOH, 98%) were purchased from Sigma-Aldrich for MWNTs functionalisation. Before use, all chemicals were passed through a chromatographic column consisting of neutral and basic aluminium oxide powders (aluminium oxide 90 (0.063–0.200 mm), activity stage I for column chromatography, Merck Millipore, Germany) and further degassed by bubbling N_2 gas for 30 minutes, in order to remove radical inhibitors and oxygen.

2.2 Functionalisation of MWNTs

2.2.1 Thermochemical grafting—The thermal activation process was carried out in a custom-made 30 mm diameter quartz tube attached to a sample flask, and the whole setup was connected to a vacuum system. In a typical experiment, 100 mg MWNTs were heated to 1000°C at a constant ramping rate of 10 °C/min under vacuum (~ 5×10^{-4}mbar), in a three-zone tube furnace (PTF 12/38/500, Lenton Ltd, UK) and held at the activation temperature for 2 hours. After the activation step, the quartz tube was slowly removed from the heating zone and allowed to cool to room temperature under vacuum. The MWNTs were then transferred to the connected round bottom flask by gravity. 8 mL of the reactant was then injected into the flask containing the thermally-activated MWNTs. The reaction mixture was stirred at room temperature overnight. The unreacted reactant was removed via filtration through a 0.45 μm pore size polytetrafluoroethylene (PTFE) membrane (Whatman, UK) under vacuum. The product was thoroughly washed with 3 × 90 mL of washing solvent, then dispersed in 90 mL of solvent and bath sonicated (USC300T, 45kHz, 80W, VWR International, USA) for 15 minutes. The filtration-sonication cycle was repeated three times in order to remove any physically absorbed reactants. The functionalised MWNTs are named by the abbreviation of the grafted polymer: e.g. P(MMA)-MWNT. The other sample codes can be found in Table 1.

2.2.2 Synthesis of P(M4-VP)-MWNT—P(4-VP)-MWNTs (20 mg) were dispersed in 10 mL of methanol (99.8%, Sigma-Aldrich) by sonication for 5 minutes; IMe (3.12 mL, 50.0 mmol) was added drop-wise, and the reaction mixture was heated to 60 °C overnight under N_2 atmosphere [45]. Afterwards, the mixture was cooled to room temperature and filtered through a 0.45 μm PTFE membrane. The MWNTs were washed with 3 × 30 mL of ethanol, then dispersed in 30 mL of ethanol and bath sonicated for 15 minutes. The filtration-sonication cycle was repeated three times in order to remove any physically absorbed reactants.

2.2.3 Synthesis of P(MAA)-MWNT—LiOH (40 mg) was dissolved in 20 mL 10:1 v/v THF/water cosolvent before adding 20 mg of P(MMA)-MWNT. The reaction mixture was bath sonicated for 5 min to obtain a good dispersion, and then stirred at room temperature overnight. Subsequently, 37% hydrochloric acid (HCl, AnalaR grade, BDH) was added

drop-wise until the pH value of the solution reached pH 2 [46]. The mixture was stirred for another 12 hours, then filtered on a 0.45 μm PTFE membrane, and washed with water (3 × 30 mL). The MWNT residue was dispersed in 30 mL of water by bath sonication for 15 minutes. The filtration-sonication cycle was repeated three times in order to remove any remaining salt and acid.

2.2.4 Acid oxidation functionalisation—In a typical reaction, 300 mg of Arkema MWNTs and 30 mL of concentrated sulphuric acid (A.R. grade, 98%, Sigma-Aldrich) mixed with nitric acid (puriss. p.a. plus, 65%, Fluka) with a volume ratio of 3:1 were heated to reflux at 120°C. After 30 minutes, the reaction solution was cooled and then diluted with 500 mL of icy water [27]. In order to remove the carbonaceous debris generated, a base wash process was carried out [26]. The acid oxidised MWNTs (AO-MWNT) were first washed with distilled water through a sintered glass filter, using a 0.45 μm PTFE membrane, until the filtrate was colourless and the pH reached that of the distilled water (~ 5.5). Subsequently, the AO-MWNT were washed with approximately 500 mL of 0.01 mol/L sodium hydroxide (NaOH, AnalaR grade, BDH, UK), until the initially dark brown filtrate ran clear. The solution was then once again washed with distilled water until the filtrate reached neutral pH. Finally, the MWNTs were washed with approximately 500 mL of 0.01 mol/L HCl (AnalaR grade, BDH, UK) and then washed to neutral pH once again.

2.3 Characterisation of MWNTs

2.3.1 Electron microscopy—MWNTs were dispersed in HPLC water by bath sonication for 5 minutes, dropped on holey carbon copper TEM grids, and pre-dried for TEM imaging. Bright-field TEM (BF-TEM) imaging was carried out on an C_s-aberration-corrected FEI Titan 80/300 with an accelerating voltage of 80kV, which is below the critical threshold energy predicted for severe knock-on damage in MWNTs [47]. A beam damage study confirmed that no visible damage to the MWNTs occurred during direct exposure to the beam with an electron dose of ~ 11000 electrons/nm^2/s for 60 minutes, in high resolution (HR)-TEM mode.

2.3.2 Thermogravimetric analysis (TGA)—TGA analyses were carried out using a Perkin Elmer Pyris 1, by heating 1.8 ± 0.2 mg MWNT samples to 100 °C, under a N_2 atmosphere (60 mL/min), and holding isothermally for 30 minutes to remove residual water and/or solvent; the temperature was then increased from 110 °C to 850 °C at a constant ramping rate of 10 °C/min under flowing N_2 (60 mL/min).

2.3.3 Zeta-potential measurement—Zeta-potential analyses were performed on a Brookhaven ZetaPALS. MWNT samples were dispersed in HPLC water with a concentration of 50 μg/mL by bath sonication for 15 minutes. The pH was adjusted using 0.1 or 0.01 M HCl/NaOH, measured by a digital pH meter (VWR sympHony™ meter, VWR International, USA).

2.3.4 Raman spectroscopy—Raman spectra (1000 – 1800 cm^{-1}) were collected on a LabRam Infinity Raman spectrometer, using a 532 nm laser (scan time 90 seconds, averagely 3 scan cycles). The D/G ratio was determined from the ratio of integrated areas

under the Raman bands at around 1350 cm^{-1} (D-band) and 1580 cm^{-1} (G-band) respectively [48]. Average values and standard deviations were obtained from five independent measurements.

2.3.5 UV–vis spectroscopy—The water compatibility of MWNTs was characterised by UV-vis spectroscopy (Lambda 950, Perkin Elmer). For water solubility tests, as-received and functionalised MWNTs were bath sonicated (45kHz, 80W, VWR International, USA) in HPLC water for 15 minutes with different initial powder loading concentrations of 100 μg/mL, 500 μg/mL, 1 mg/mL and 2 mg/mL. MWNT aggregates were settled by centrifugation for 15 minutes at 10, 000 g. For cell medium compatibility tests, as-received and functionalised MWNTs were bath sonicated (45kHz, 80W, VWR International) in serum-free DCCM-1 tissue culture medium (Biological Industries Israel Beit-Haemek Ltd, Israel) for 15 minutes with 2 mg/mL initial powder loading concentrations. The supernatant was carefully decanted and the concentration of grafted MWNTs determined by UV absorbance and application of the Beer-Lambert law, $A = \varepsilon \times c \times d$, where $A$is the measured UV absorbance, ε is the extinction coefficient (35.10 $mL \cdot mg^{-1} \cdot cm^{-1}$ for Arkema MWNTs at 800 nm [49]) and d is the light path length (1 cm cuvette length, in this study).

2.4 Endotoxin assay

Although, the thermal activation process guaranteed the sterility of the activated MWNTs [50], after synthesis the MWNTs were handled in a laminar flow cabinet to maintain sterility. An endotoxin assay was performed using LAL Chromogenic Endotoxin Quantitation Kit (Thermo Scientific, UK). All the glassware used for the CNT functionalisation, washing steps and LAL assay were used after oven sterilization at 120°C for at least 2 h.

2.5 Cell viability assay

2.5.1 Cell culture—Human TT1 cells are an immortal epithelial type I-like cell line derived from primary human AT2 cells [51]. TT1 cells were seeded at a density of 8,000 cells per well in 96 well plates. The TT1 cells were cultured in DCCM-1 medium supplemented with 10% newborn calf serum (NCS), 100 U/ml penicillin, 100μg/ml streptomycin and 2mM glutamine. Once the cells reached confluence they were serum starved for 24 hours prior to MWNT exposure.

2.5.2 MWNT exposures—Immediately prior to cell exposures, MWNTs were suspended in serum-free DCCM-1 at a concentration of 1 mg/mL, vortexed for 1 minute and then sonicated in a water bath (42 kHz, 135 W, VWR International, USA) for 10 minutes. This stock solution was diluted in DCCM-1 to the required doses (0 – 50 μg/mL) and sonicated briefly prior to cell exposure. The cells were exposed to MWNTs with required doses (0 – 50 μg/mL) for 24 hours. All exposures were performed in triplicate.

2.5.3 MTS assay—MTS is a tetrazolium compound that can be reduced by dehydrogenase enzymes within living cells demonstrating metabolic activity and cell viability. Such reduction in the presence of an electron coupling reagent, phenazineethosulfate (MPS), results in the production of formazan which is soluble in tissue culture medium; the

absorbance of this formazan product was measured at a wavelength of 492 nm using spectrophotometer Following exposure to the MWNTs, cells were washed with PBS and incubated with medium containing MTS reagent (CellTiter 96® AQueous One Solution Assay, Promega, USA) according to the manufacturer's protocol.

2.5.4 LDH assay—LDH is a soluble cytosolic enzyme, the release of which is associated with the damage of cell plasma membrane and cell necrosis. The LDH assay was performed on the cell supernatants collected following the exposure, according to the manufacturer's instructions (Roche Applied Science, Indianapolis, USA). To control for residual particles, MWNT agglomerates were removed by centrifugation at 3000 rpm and the absorbance of the medium was determined at 492 nm prior to the LDH assay. The background absorbance of the conditioned medium was subtracted from the final absorbance value obtained upon analysis.

2.6 IL6/IL8 detection assay

Interleukin 8 (IL8) and interleukin 6 (IL6) are chemokines that can be produced by epithelial cells and are often cited as inflammatory mediators. Cell supernatants were collected from experiments performed in an identical manner to those described above and the concentration the inflammatory mediators IL-6 and IL-8 was determined using a sandwich ELISA according to the manufacturer's protocol (R&D Systems, Ltd, UK).

2.7 TEM Cell uptake study

Functionalised MWNTs were first sonicated in a water bath (45kHz, 80W, VWR International, USA) in HPLC water for 15 minutes with initial powder loading concentration of 1 mg/mL. MWNT aggregates were pelleted out by centrifugation for 15 minutes at 10,000 g, and the supernatants, containing dispersed MWNTs were used for cell exposure studies. TT1 cells were seeded on 24 well plates to reach 100% confluence, as described above, and cells were then serum starved for 24 hours before exposure to MWNT suspensions at a concentration of 5 μg/mL. After 24 h exposure, the cells were rinsed with HEPES buffer and were then fixed with 2.5% glutaraldehyde for 1 hours. The samples were post-fixed in 1% osmium tetroxide for 30 minutes. Each sample was then dehydrated in a graded ethanol series of 50%, 70%, 90% and 100% (volume ratio of ethanol to DI-H_2O) ethanol for 15 minutes (3×) each, all at room temperature. After dehydration, samples were progressively infiltrated with 25% and 50% araldite resin/ethanol solution (Agar Scientific, UK) and each well was incubated for 15 minutes (×2), at room temperature, followed by infiltration in 100% resin. The specimens were then embedded into resin. The embedded cell monolayers were cut using an ultramicrotome with a 35 degree diamond knife to a thickness of 50–100nm. The obtained sections were observed in a JEOL 2000 transmission electron microscope operated at an accelerating voltage of 80 kV. Multiple cells (>100 per sample) from three cell exposures were surveyed by TEM.

3 Results and Discussion

The functionalisation of MWNTs was carried out using an adaptation of the solvent-free thermochemical 'grafting from' protocols reported previously [35], taking advantage of

preexisting surface oxides on as-received MWNTs rather than an explicit oxidation step. The concentration of oxygen on the surface of typical ~10 nm (diameter) CVD MWNTs, as synthesised, is approximately one oxygen per 100–250 surface carbons [36]; some fraction of these groups will be suitable for generating radicals upon activation.

To prepare negatively-charged MWNTs (P(MAA)-MWNT), hydrophobic methyl methacrylate grafted MWNTs were hydrolysed in alkaline solution in order to generate carboxylic acid groups. 4-VP is a weak base [52], therefore, P(4-VP)-MWNT can provide a positive surface charge when protonated; in order to obtain more stable charges on the surface of MWNTs, a quaternisation reaction was carried out, through methylation of the pyridyl groups, to introduce positive charge onto the surface of the MWNTs (Scheme 1).

3.1 TGA analysis

The grafting ratio and degrees of polymerisation were characterised based on TGA analysis. As shown in Figure 1 and SI-Figure 1S, the TGA profile of grafted MWNTs displayed weight losses in the range 200–800 °C, in contrast to as-received (AR) and non-grafted thermal treated control (TTC) MWNTs, which can be attributed to the decomposition of the grafted organic oligomers. This step indicates the successful oligomer/polymer grafting. The grafting ratio was calculated based on the difference between the weight loss of the functionalised MWNTs and a thermally treated control (TTC) MWNTs, in order to exclude any effect of minor volatile/adsorbed impurities within the as-received (AR) MWNTs. The TTC sample was obtained using same activation protocol as functionalisation, but exposing activated MWNTs to air rather than a monomer, at ambient temperatures. This process allows the surface to be re-oxidised at the original oxide defect sites, providing a simple baseline for the grafted products [49]. As a further control, to determine the number of active sites, the MWNTs were grafted with the non-polymerisable reagent 1-iodododecane (IDD). The grafting density and degree of polymerisation were then calculated (Table 1), assuming that IDD reacts stoichiometrically with all active radical sites, and the polymerisation processes is initiated at a radical site but can terminate anywhere on the MWNT surface.

The grafting ratio of the P(MMA)-MWNT (3.9 wt%) decreased slightly after the hydrolysis treatment (3.4 wt%), due to the loss of methyl groups. The grafting ratio of 4-VP-grafted MWNTs was 4.1 wt%, and the degree of polymerisation was very similar to that of P(MMA)-MWNT. TGA of the quaternised product retained the features of the P(4-VP)-MWNTs, associated with the combustion of the grafted oligomer, with an additional loss at around 200°C, attributed to the methyl group and the associated iodide counterion. In order to account for the possible interaction of IMe with remaining surface oxides not involved in the grafting reaction, a methylated control sample (IMe-TTC) was prepared. Results (SI-Figure 2S) indicated a small degree of secondary methylation (3.8 wt%), with the loss of quaternised IMe (5.3 wt%) at about 270 °C and remaining P(4-VP) framework (3.4 wt%), in the ranges expected. The higher grafting ratio of PEGylated MWNT, 18.3 wt%, is attributed to the high molecular weight of side chain of PEGMA monomer, and the degree of polymerization is very similar to other monomers (Table 1).

3.2 MWNT water compatibility study

The functionalised MWNTs showed significantly enhanced water compatibility compared to AR-MWNT, as indicated by the dark color of the supernatant solutions (Figure 2a) after centrifugation (10, 000g, 15 minutes). The improvement after grafting is also illustrated by the individualised MWNTs visible by TEM, as compared to the AR-MWNT which remain aggregated after similar processing in water (Figure 2b). The suspended concentration in HPLC water provides a quantitative measure of water compatibility, but it is important to understand the effect of increasing the amount of dry material supplied (Figure 2c). Initially, the suspended concentration increases rapidly (P(M4-VP) > P(PEGMA) > P(MAA), indicating a minimum yield of dispersed, individualised species of around 17, 15 and 7% respectively. Subsequently, the MWNTs supernatant concentrations saturate, indicating the water solubility of the modified MWNT species. Taking the plateau values obtained at 2 mg/mL, the PEGMA-MWNT showed a much improved water compatibility compared to the pristine MWNTs, with a supernatant concentration of ~60 μg/mL attributed to the high grafting ratio and the steric stabilisation effects of the relatively bulky and hydrophilic PEG side chains. The P(4-VP)-MWNT offered a more modest improvement; in this case, the stabilisation is likely to depend on the electrostatic contribution of the protonated pyridyl groups. However, since the pyridyl group is a weak base [52], there is only limited protonation, and hence low stability, near pH 7. In order to increase the stability, the pyridyl groups were methylated to create a positive charge and a stronger columbic repulsion. The success of this strategy is illustrated by the 4-fold increase in P(M4-VP)-MWNT solubility to ~ 70 μg/mL. P(MMA)-MWNT showed very low water stability, similar to the parent AR-MWNT, as PMMA itself is not water-soluble. After the introduction of carboxyl acid groups through hydrolysis of grafted P(MMA), the stability of MWNTs was significantly increased to 30 μg/mL for P(MAA)-MWNT, again indicating the success of the intended reaction. For the P(MAA)-MWNT, P(M4-VP)-MWNT and P(PEGMA)-MWNT samples, less than 20% of MWNTs precipitated out after 2 weeks, as determined by UV-vis analysis, providing good stability for *in vitro* experiments.

3.3 Zeta potential analysis

The zeta potential analysis further confirmed successful grafting of the MWNTs with anionic, non-ionic and cationic oligomers (Figure 2d). The AR-MWNT and thermal treated controls are weakly acidic, with an iso-electric point (IEP) of 5.0 and 4.3, as expected given the surface oxides, including carboxylic acid groups, present on the surface of such MWNTs [53]. The MAA modification increases the concentration of carboxylic acid groups, with a similar pKa, such that the IEP (4.3) is approximately unchanged, but the plateau zeta potential is greater in magnitude. The grafted PEGMA is non-ionic so does not shift the IEP of the baseline groups; however, some of the oxygen species were consumed by the grafting process, leading to a lower plateau potential. Nevertheless, it is worth re-emphasising that the water compatibility is driven by the non-ionic PEG chains. The 4-VP functionalised systems introduce positively-charged groups, shifting the IEP to higher pH. By introducing a positive charge through quaternisation, the IEP of P(M4-VP)-MWNT was successfully increased to about pH 9.8.

3.4 HRTEM and Raman spectroscopy analysis

The thermochemically-grafted MWNTs were undamaged by the process, as anticipated. The two main Raman peaks for MWNTs, at around 1580 cm^{-1} (G) and 1350 cm^{-1} (D), are associated with graphitic quality and defects, respectively. The integrated peak area ratio (D/G) gives a semi-quantitative indication of the purity / defect density. The D/G ratios of the products (Table 2, SI-Figure 3S) were unchanged, within error, relative to the as-received starting material value of 1.09 ± 0.03. Furthermore, HRTEM (Figure 3a–d) showed no discernible change in the structure of the tubes, including no change in surface crystallinity, nanotube dimensions, or graphitic interlayer spacing (0.35 ± 0.01 nm). The grafted organic oligomers cannot be directly imaged due to their conformational freedom and high beam sensitivity. In total contrast to the thermochemical process, the liquid phase acid oxidation significantly damaged the framework of the MWNTs. Even after base washing to remove debris [26], the D/G ratio increased by 46% (SI-Figure 3S). By HRTEM (Figure 3e), obvious MWNTs framework damage, such as peeling and thinning of MWNTs walls (marked by arrows and oval) and generation of holes (circled area), was observed. This framework damage will inevitably effect the intrinsic properties of MWNTs, likely altering their toxicity and fate *in vivo*. Acid oxidised MWNTs are, therefore, not good models for studying the biological interactions of the majority of commercially-produced materials.

3.5 Cytotoxicity study

Before assessing the cytotoxicity of *f*-MWNTs, the endotoxin content of the samples was assessed. The results (SI-Figure 4S) showed that the panel of *f*-MWNTs were negative for endotoxin by normal standards, demonstrating that the thermochemical functionalisation treatment and post-functionalisation reactions do not introduce any significant level of endotoxin; in fact, the high temperature treatment provides useful sterilization.

The cytotoxicity of MWNTs on TT1 cells was assessed using MTS (Figure 4a) and LDH (Figure 4b) assays. None of the MWNTs showed any significant TT1 cell cytotoxicity after 24 hours exposure to concentrations up to 50 μg/mL (Figure 4a). Only a slight toxic effect of AR MWNTs was observed (less than 10% cell death, n=3 replicates). The low cell viability damage suggested by the MTS assay was confirmed by LDH assays (Figure 4b), showing no detectable cell death.

However, exposure of TT1 cells to MWNTs suppressed IL-6 (Figure 4c and d) and IL-8 release in a dose-dependent fashion. All of the MWNTs, even the lowest dose of 1 μg/ml, caused some inhibition; the effect became highly significant at higher doses, with values falling to a third of that of control. Cationic P(M4-VP) may be slightly less inhibitory than the rest of the panel, but the difference was not significant. A similar inflammatory mediator suppression effect was reported following exposure of A549 adenocarcinoma cells and a single subject sample of primary NHBE human airway lung epithelial cells to single wall carbon nanotubes (SWNTs), which led to the suppression of IL-6, IL-8 and MCP-1, which was further suppressed by addition of dipalmitoylphosphatidylcholine (DPPC) [54]. In contrast, exposure of the BEAS 2B human airway cell line to a highly purified vapour-grown multiwalled carbon fiber, HTT2800 [55], or commercial MWNT synthesized by

catalytic chemical vapor deposition (CCVD) [56], caused increased IL-6 and IL-8 release. As different cell lines, as well as carbon nanomaterials of different dimensions and surface functionalization were studied, it is difficult to make a comparison with these contrasting literature results. Importantly in the current study, the AR-MWNTs have been surface modified to enhance dispersibility and modify bioreactivity and tested using highly relevant, well characterised, human lung alveolar epithelial cells (rather than airway epithelium and cancer cells). One key question, however, is to what extent these cells interact with the test panel of MWNTs.

3.6 TEM cell uptake study

Consequently, a TEM study was carried out to investigate alveolar epithelial cell interactions with cationic, anionic and non-ionic MWNTs. The stable water dispersions of individual *f*-MWNTs (see Figure 2a) provide an excellent route for cell exposure. In contrast, on exposing TT1 cells directly to uncentrifuged suspensions of AR-MWNT containing agglomerates due to its limited water dispensability, the majority of AR-MWNTs were localized in TT1 cells as large clusters inside cellular vesicles, indicating internalisation via endocytic pathways (SI-Figure 5S). Uptake of *f*-MWNTs by TT1 cells proceeded by a variety of mechanisms (Figure 5). The non-ionic P(PEGMA)-MWNTs were observed inside vesicular structures (Figure 5a), possibly utilizing energetic endocytosis pathways [57]. A collection of P(PEGMA)-MWNTs were also in the process of being taken up by macropinocytosis, as featured by the presence of large protrusions of the plasma membrane (> 1 μm) around the MWNTs [58] (Figure 5a). Other types of endocytic uptake were observed (see Figure 5b, marked by arrows) involving relatively smaller sized vesicles, compared to those involved in macropinocytosis. Individual P(PEGMA)-MWNTs were also present inside the cytoplasm (Figure 5a, circled and Figure 5c). These individual MWNTs might have entered the cell cytoplasm by directly penetrating cell membranes [59, 60], as indicated by arrows in Figure 5c. There was also a surface charge effect on the interaction of these functionalized MWNTs with epithelial cells. Thus, a large population of anionic, negatively charged P(MAA)-MWNTs were observed localised inside vesicular structures (Figure 5d–e), while a sub-population of individual P(MAA)-MWNTs were also detected within the cytoplasm (Figure 5d, circled). Macropinocytosis (Figure 5d, arrow) and other endocytic mechanisms were also observed for this type of MWNTs (Figure 5e, arrow). Furthermore, P(MAA)-MWNTs, were frequently aligned parallel to, and did not insert into, the plasma membrane, possibly due to the electrostatic repulsion of negatively charge MWNTs with the negatively charged plasma membrane (Figure 5f, SI-Figure 6S). The cationic, positively charged M(4-VP)-grafted MWNTs also distributed to both the cytoplasm and endocytic vesicular structures (Figure 5g–i). However, P(M4-VP)-MWNT exhibited more frequent contact with the plasma membrane than the other MWNTs. The M(4-VP)-MWNTs inserted into the plasma membrane with both high and low contact angles, presumably due to electrostatic attraction [61–63].

3.7 Wider context

The versatile, scalable functionalization method used in this paper can also be applied for other modifications of MWNTs, in order to change their surface charge or functional character. Non-cytotoxic MWNTs with defined surface charges have many perceived

biological applications ranging from acting as intracellular transporters for various therapeutic and diagnostic agents to cell growth substrates or tissue scaffolds [64]. Furthermore, water dispersible MWNTs may be used to simplify processing in a range of applications from printing conductive inks, to assembling filters and electrodes. In many cases, avoiding MWNT damage, and the property degradation associated with acid oxidation, as well as improving the scalability of the chemistry, will be significantly advantageous. Controlled and stably grafted surface charge provides options to use electrostatically-driven techniques such as layer-by-layer (LBL) assembly and electrophoretic deposition (EPD) [65]. The versatile chemistry described allows model sets of surface-modified MWNTs to be prepared without changing dimensions or structure; for example, as shown here, the structural integrity of commercially-grown MWNTs can be retained whilst producing water-stable dispersions with different surface character. Understanding this type of industrial MWNTs is particularly important as annual production capacity is in the order of thousands of tons [66], vastly exceeding any other nanotube material. The methods presented in this study are also likely to be suitable for the functionalisation of other carbon-related materials such as carbon black and graphene, which may thus provide useful controls for exploring geometric effects.

4. Conclusions

In this study, a thermochemical approach was successfully applied for preparation of water-compatible MWNTs, stabilised by cationic, anionic, or non-ionic grafted species. In contrast to traditional acid oxidation protocols, the thermochemical method has a significant advantage of minimising the damage to the nanotube framework. The functionalised MWNTs showed significantly enhanced water compatibility; the concentration of individualized, grafted MWNTs in water ranged from ~30–70 μg/mL, high enough for most biological research purposes. None of the MWNTs showed significant cytotoxicity toward human alveolar epithelial cells (<10%). In addition, exposure of TT1 cells to MWNTs led to the suppression of IL-6 and IL-8, suggesting that they would not trigger an inflammatory response if deposited within the respiratory units. Nevertheless, TEM showed marked uptake of all types of MWNTs by TT1 cells. MWNTs were found residing in cellular vesicular structures and cytoplasm, with both endocytic uptake pathways and direct penetration of cell surface membrane implicated as important cellular entry mechanisms. Surface charge appears to be important, since cationic MWNTs showed greater direct interaction with cell membranes, involving more substantial direct penetration of the membranes than anionic MWNTs. These fundamental factors controlling nanomaterial-cell interactions must be understood, in order to build up a generally applicable model.

Supplementary Material

Refer to Web version on PubMed Central for supplementary material.

Acknowledgments

The authors would like to thank NIEHS (grant# U19ES019536) for the funding of this project. AP acknowledges an ERC starting grant (CNTBBB project number 257182) for supporting AEG and SC. TT acknowledges funding

from Leverhulme for supporting PR and Medical Research Council for supporting ES. However, the views expressed in this paper are solely of the authors and do not necessarily reflect those of the funding agencies.

Reference

1. Gagner JE, Shrivastava S, Qian X, Dordick JS, Siegel RW. Engineering nanomaterials for biomedical applications requires understanding the nano-bio interface: a perspective. J Phys Chem Lett. 2012; 3:3149–3158.
2. Shannahan JH, Brown JM, Chen R, Ke PC, Lai XY, Mitra S, et al. Comparison of nanotube-protein corona composition in cell culture media. Small. 2013; 9:2171–2181. [PubMed: 23322550]
3. Moon HK, Lee SH, Choi HC. *In vivo* near-infrared mediated tumor destruction by photothermal effect of carbon nanotubes. Acs Nano. 2009; 3:3707–3713. [PubMed: 19877694]
4. Wang L, Shi JJ, Zhang HL, Li HX, Gao Y, Wang ZZ, et al. Synergistic anticancer effect of RNAi and photothermal therapy mediated by functionalized single-walled carbon nanotubes. Biomaterials. 2013; 34:262–274. [PubMed: 23046752]
5. Bhirde AA, Patel V, Gavard J, Zhang GF, Sousa AA, Masedunskas A, et al. Targeted killing of cancer Cells *in vivo* and *in vitro* with EGF-directed carbon nanotube-based drug delivery. Acs Nano. 2009; 3:307–316. [PubMed: 19236065]
6. Chen ML, He YJ, Chen XW, Wang JH. Quantum dots conjugated with Fe_3O_4-filled carbon nanotubes for cancer-targeted imaging and magnetically guided drug delivery. Langmuir. 2012; 28:16469–16476. [PubMed: 23131026]
7. de la Zerda A, Liu ZA, Bodapati S, Teed R, Vaithilingam S, Khuri-Yakub BT, et al. Ultrahigh sensitivity carbon nanotube agents for photoacoustic molecular imaging in living mice. Nano Lett. 2010; 10:2168–2172. [PubMed: 20499887]
8. Delogu LG, Vidili G, Venturelli E, Menard-Moyon C, Zoroddu MA, Pilo G, et al. Functionalized multiwalled carbon nanotubes as ultrasound contrast agents. P Natl Acad Sci USA. 2012; 109:16612–16617.
9. Zhang XY, Hu WB, Li J, Tao L, Wei Y. A comparative study of cellular uptake and cytotoxicity of multi-walled carbon nanotubes, graphene oxide, and nanodiamond. Toxicol Res-Uk. 2012; 1:62–68.
10. Nel A, Xia T, Meng H, Wang X, Lin SJ, Ji ZX, et al. Nanomaterial toxicity testing in the 21st century: use of a predictive toxicological approach and high-throughput screening. Acc Chem Res. 2013; 46:607–621. [PubMed: 22676423]
11. Li JQ, Zhang Q, Li H, Chan-Park MB. Influence of triton X-100 on the characteristics of carbon nanotube field-effect transistors. Nanotechnology. 2006; 17:668–673.
12. Duan WH, Wang Q, Collins F. Dispersion of carbon nanotubes with SDS surfactants: a study from a binding energy perspective. Chem Sci. 2011; 2:1407–1413.
13. Li MH. Effects of nonionic and ionic surfactants on survival, oxidative stress, and cholinesterase activity of planarian. Chemosphere. 2008; 70:1796–1803. [PubMed: 17905407]
14. Ma G, Allen HC. New insights into lung surfactant monolayers using vibrational sum frequency generation spectroscopy. Photochem Photobiol. 2006; 82:1517–1529. [PubMed: 16930094]
15. Huang YY, Terentjev EM. Dispersion of carbon nanotubes: mixing, sonication, stabilization, and composite properties. Polymers-Basel. 2012; 4:275–295.
16. Bussy C, Pinault M, Cambedouzou J, Landry MJ, Jegou P, Mayne-L'hermite M, et al. Critical role of surface chemical modifications induced by length shortening on multi-walled carbon nanotubes-induced toxicity. Part Fibre Toxicol. 2012; 9:46. [PubMed: 23181604]
17. Baati R, Ihiawakrim D, Mafouana RR, Ersen O, Dietlin C, Duportail G. Hexahistidine-Tagged single-walled carbon nanotubes (His6-tagSWNTs): a multifunctional hard template for hierarchical directed self-assembly and nanocomposite construction. Adv Funct Mater. 2012; 22:4009–4015.
18. Guo XF. Single-molecule electrical biosensors based on single-walled carbon nanotubes. Adv Mater. 2013; 25:3397–3408. [PubMed: 23696446]
19. Shaffer MSP, Fan X, Windle AH. Dispersion and packing of carbon nanotubes. Carbon. 1998; 36:1603–1612.

20. Wang YB, Iqbal Z, Mitra S. Rapidly functionalized, water-dispersed carbon nanotubes at high concentration. J Am Chem Soc. 2006; 128:95–99. [PubMed: 16390136]
21. Gonzalez-Dominguez JM, Gonzalez M, Anson-Casaos A, Diez-Pascual AM, Gomez MA, Martinez MT. Effect of various aminated single-walled carbon nanotubes on the epoxy cross-linking reactions. J Phys Chem C. 2011; 115:7238–7248.
22. Li KD, Zhang C, Du ZJ, Li HQ, Zou W. Preparation of humidity-responsive antistatic carbon nanotube/PEI nanocomposites. Synt Met. 2012; 162:2010–2015.
23. Tchoul MN, Ford WT, Lolli G, Resasco DE, Arepalli S. Effect of mild nitric acid oxidation on dispersability, size, and structure of single-walled carbon nanotubes. Chem Mater. 2007; 19:5765–5772.
24. Datsyuk V, Kalyva M, Papagelis K, Parthenios J, Tasis D, Siokou A, et al. Chemical oxidation of multiwalled carbon nanotubes. Carbon. 2008; 46:833–840.
25. Verdejo R, Lamoriniere S, Cottam B, Bismarck A, Shaffer M. Removal of oxidation debris from multi-walled carbon nanotubes. Chem Commun. 2007:513–515.
26. Fogden S, Verdejo R, Cottam B, Shaffer M. Purification of single walled carbon nanotubes: The problem with oxidation debris. Chem Phys Lett. 2008; 460:162–167.
27. Cho J, Inam F, Reece MJ, Chlup Z, Dlouhy I, Shaffer MSP, et al. Carbon nanotubes: do they toughen brittle matrices? J Mater Sci. 2011; 46:4770–4779.
28. Wang RH, Mikoryak C, Li SY, Bushdiecker D, Musselman IH, Pantano P, et al. Cytotoxicity screening of single-walled carbon nanotubes: detection and removal of cytotoxic contaminants from carboxylated carbon nanotubes. Mol Pharmaceut. 2011; 8:1351–1361.
29. Stefani D, Paula AJ, Vaz BG, Silva RA, Andrade NF, Justo GZ, et al. Structural and proactive safety aspects of oxidation debris from multiwalled carbon nanotubes. J Hazard Mater. 2011; 189:391–396. [PubMed: 21429665]
30. Heister E, Lamprecht C, Neves V, Tilmaciu C, Datas L, Flahaut E, et al. Higher dispersion efficacy of functionalized carbon nanotubes in chemical and biological environments. Acs Nano. 2010; 4:2615–2626. [PubMed: 20380453]
31. Yamashita T, Yamashita K, Nabeshi H, Yoshikawa T, Yoshioka Y, Tsunoda S, et al. Carbon nanomaterials: efficacy and safety for nanomedicine. Materials. 2012; 5:350–363.
32. Li R, Wang X, Ji Z, Sun B, Zhang H, Chang CH, et al. Surface charge and cellular processing of covalently functionalized multiwall carbon nanotubes determine pulmonary toxicity. Acs Nano. 2013; 7:2352–2368. [PubMed: 23414138]
33. Tagmatarchis N, Prato M. Functionalization of carbon nanotubes via 1,3-dipolar cycloadditions. J Mater Chem. 2004; 14:437–439.
34. Hodge SA, Fogden S, Howard CA, Skipper NT, Shaffer MSP. Electrochemical processing of discrete single-walled carbon nanotube anions. Acs Nano. 2013; 7:1769–1778. [PubMed: 23336405]
35. Menzel R, Tran MQ, Menner A, Kay CWM, Bismarck A, Shaffer MSP. A versatile, solvent-free methodology for the functionalisation of carbon nanotubes. Chem Sci. 2010; 1:603–608.
36. Tessonnier JP, Rosenthal D, Hansen TW, Hess C, Schuster ME, Blume R, et al. Analysis of the structure and chemical properties of some commercial carbon nanostructures. Carbon. 2009; 47:1779–1798.
37. Castranova V, Schulte PA, Zumwalde RD. Occupational nanosafety considerations for carbon nanotubes and carbon nanofibers. Acc Chem Res. 2013; 46:642–649. [PubMed: 23210709]
38. Morimoto Y, Horie M, Kobayashi N, Shinohara N, Shimada M. Inhalation toxicity assessment of carbon-based nanoparticles. Acc Chem Res. 2013; 46:770–781. [PubMed: 22574947]
39. Murphy FA, Schinwald A, Poland CA, Donaldson K. The mechanism of pleural inflammation by long carbon nanotubes: interaction of long fibres with macrophages stimulates them to amplify pro-inflammatory responses in mesothelial cells. Part Fibre Toxicol. 2012; 9:8. [PubMed: 22472194]
40. Murphy FA, Poland CA, Duffin R, Donaldson K. Length-dependent pleural inflammation and parietal pleural responses after deposition of carbon nanotubes in the pulmonary airspaces of mice. Nanotoxicology. 2013; 7:1157–1167. [PubMed: 22812632]

41. Maynard RL, Donaldson K, Tetley TD. Type 1 pulmonary epithelial cells: a new compartment involved in the slow phase of particle clearance from alveoli. Nanotoxicology. 2013; 7:350–351. [PubMed: 22292454]
42. Crapo JD, Young SL, Fram EK, Pinkerton KE, Barry BE, Crapo RO. Morphometric characteristics of cells in the alveolar region of mammalian lungs. Am Rev Respir Dis. 1983; 128:S42–S46. [PubMed: 6881707]
43. Isakson BE, Seedorf GJ, Lubman RL, Boitano S. Heterocellular cultures of pulmonary alveolar epithelial cells grown on laminin-5 supplemented matrix. In Vitro Cell Dev-An. 2002; 38:443–449.
44. Shimada A, Kawamura N, Okajima M, Kaewamatawong T, Inoue H, Morita T. Translocation pathway of the intratracheally instilled ultrafine particles from the lung into the blood circulation in the mouse. Toxicol Pathol. 2006; 34:949–957. [PubMed: 17178695]
45. Alunni S, Laureti V, Ottavi L, Ruzziconi R. Catalysis of the beta-elimination of HF from isomeric 2-fluoroethylpyridines and 1-methyl-2-fluoroethylpyridinium salts. Proton-activating factors and methyl-activating factors as a mechanistic test to distinguish between concerted E2 and E1cb irreversible mechanisms. J Org Chem. 2003; 68:718–725. [PubMed: 12558390]
46. Runyon SP, Brieaddy LE, Mascarella SW, Thomas JB, Navarro HA, Howard JL, et al. Analogues of (3R)-7-Hydroxy-N-[(1S)-1-{[(3R,4R)-4-(3-hydroxyphenyl)-3,4-dimethyl-1-piperidinyl]methyl}-2-methylpropyl)-1,2,3,4-tetrahydro-3-isoquinolinecarboxamide (JDTic). Synthesis and in Vitro and in Vivo Opioid Receptor Antagonist Activity. J Med Chem. 2010; 53:5290–5301. [PubMed: 20568781]
47. Li SP, Wu W, Campidelli S, Sarnatskaia V, Prato M, Tridon A, et al. Adsorption of carbon nanotubes on active carbon microparticles. Carbon. 2008; 46:1091–1095.
48. Delhaes P, Couzi M, Trinquecoste M, Dentzer J, Hamidou H, Vix-Guterl C. A comparison between Raman spectroscopy and surface characterizations of multiwall carbon nanotubes. Carbon. 2006; 44:3005–3013.
49. Tran MQ, Tridech C, Alfrey A, Bismarck A, Shaffer MSP. Thermal oxidative cutting of multi-walled carbon nanotubes. Carbon. 2007; 45:2341–2350.
50. Delogu LG, Stanford SM, Santelli E, Magrini A, Bergamaschi A, Motamedchaboki K, et al. Carbon nanotube-based nanocarriers: the importance of keeping it clean. J Nanosci Nanotechno. 2010; 10:5293–5301.
51. Kemp SJ, Thorley AJ, Gorelik J, Seckl MJ, O'Hare MJ, Arcaro A, et al. Immortalization of human alveolar epithelial cells to investigate nanoparticle uptake. Am J Respir Cell Mol Biol. 2008; 39:591–597. [PubMed: 18539954]
52. Franck-Lacaze L, Sistat P, Huguet P. Determination of the pK(a) of poly (4-vinylpyridine)-based weak anion exchange membranes for the investigation of the side proton leakage. J Membr Sci. 2009; 326:650–658.
53. Menendez JA, Phillips J, Xia B, Radovic LR. On the modification and characterization of chemical surface properties of activated carbon: In the search of carbons with stable basic properties. Langmuir. 1996; 12:4404–4410.
54. Herzog E, Byrne HJ, Casey A, Davoren M, Lenz AG, Maier KL, et al. SWCNT suppress inflammatory mediator responses in human lung epithelium *in vitro*. Toxicol Appl Pharmacol. 2009; 234:378–390. [PubMed: 19041333]
55. Tsukahara T, Haniu H. Cellular cytotoxic response induced by highly purified multi-wall carbon nanotube in human lung cells. Mol Cell Biochem. 2011; 352:57–63. [PubMed: 21298324]
56. Hirano S, Fujitani Y, Furuyama A, Kanno S. Uptake and cytotoxic effects of multi-walled carbon nanotubes in human bronchial epithelial cells. Toxicol Appl Pharm. 2010; 249:8–15.
57. Mu QX, Broughton DL, Yan B. Endosomal leakage and nuclear translocation of multiwalled carbon nanotubes: developing a model for cell uptake. Nano Lett. 2009; 9:4370–4375. [PubMed: 19902917]
58. Conner SD, Schmid SL. Regulated portals of entry into the cell. Nature. 2003; 422:37–44. [PubMed: 12621426]

59. Shi XH, von dem Bussche A, Hurt RH, Kane AB, Gao HJ. Cell entry of one-dimensional nanomaterials occurs by tip recognition and rotation. Nat Nanotechnol. 2011; 6:714–719. [PubMed: 21926979]

60. Al-Jamal KT, Nerl H, Muller KH, Ali-Boucetta H, Li SP, Haynes PD, et al. Cellular uptake mechanisms of functionalised multi-walled carbon nanotubes by 3D electron tomography imaging. Nanoscale. 2011; 3:2627–2635. [PubMed: 21603701]

61. Pantarotto D, Briand JP, Prato M, Bianco A. Translocation of bioactive peptides across cell membranes by carbon nanotubes. Chem Commun. 2004:16–17.

62. Hauck TS, Ghazani AA, Chan WCW. Assessing the effect of surface chemistry on gold nanorod uptake, toxicity, and gene expression in mammalian cells. Small. 2008; 4:153–159. [PubMed: 18081130]

63. Nan AJ, Bai X, Son SJ, Lee SB, Ghandehari H. Cellular uptake and cytotoxicity of silica nanotubes. Nano Lett. 2008; 8:2150–2154. [PubMed: 18624386]

64. Heister E, Brunner EW, Dieckmann GR, Jurewicz I, Dalton AB. Are carbon nanotubes a natural solution? Applications in biology and medicine. Acs Appl Mater Inter. 2013; 5:1870–1891.

65. Boccaccini AR, Cho J, Roether JA, Thomas BJC, Minay EJ, Shaffer MSP. Electrophoretic deposition of carbon nanotubes. Carbon. 2006; 44:3149–3160.

66. De Volder MFL, Tawfick SH, Baughman RH, Hart AJ. Carbon nanotubes: present and future commercial applications. Science. 2013; 339:535–539. [PubMed: 23372006]

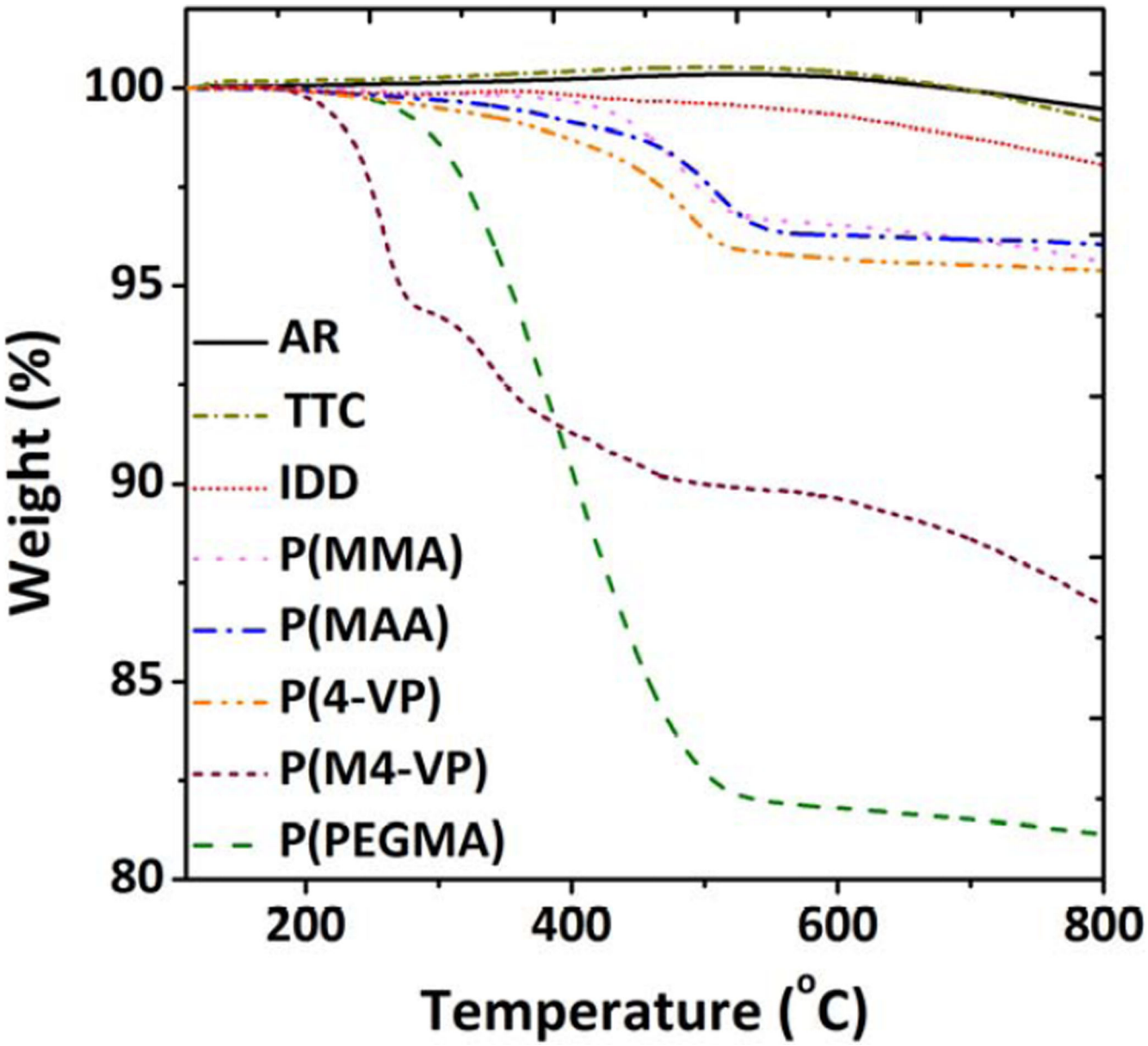

Figure 1.

TGA weight loss profiles of as received (AR) MWNTs, thermal treated control (TTC) MWNTs and various functionalised MWNTs (*f*-MWNT), heated in N_2 atmosphere at 10°C/min ramping rate from 100 °C to 800 °C.

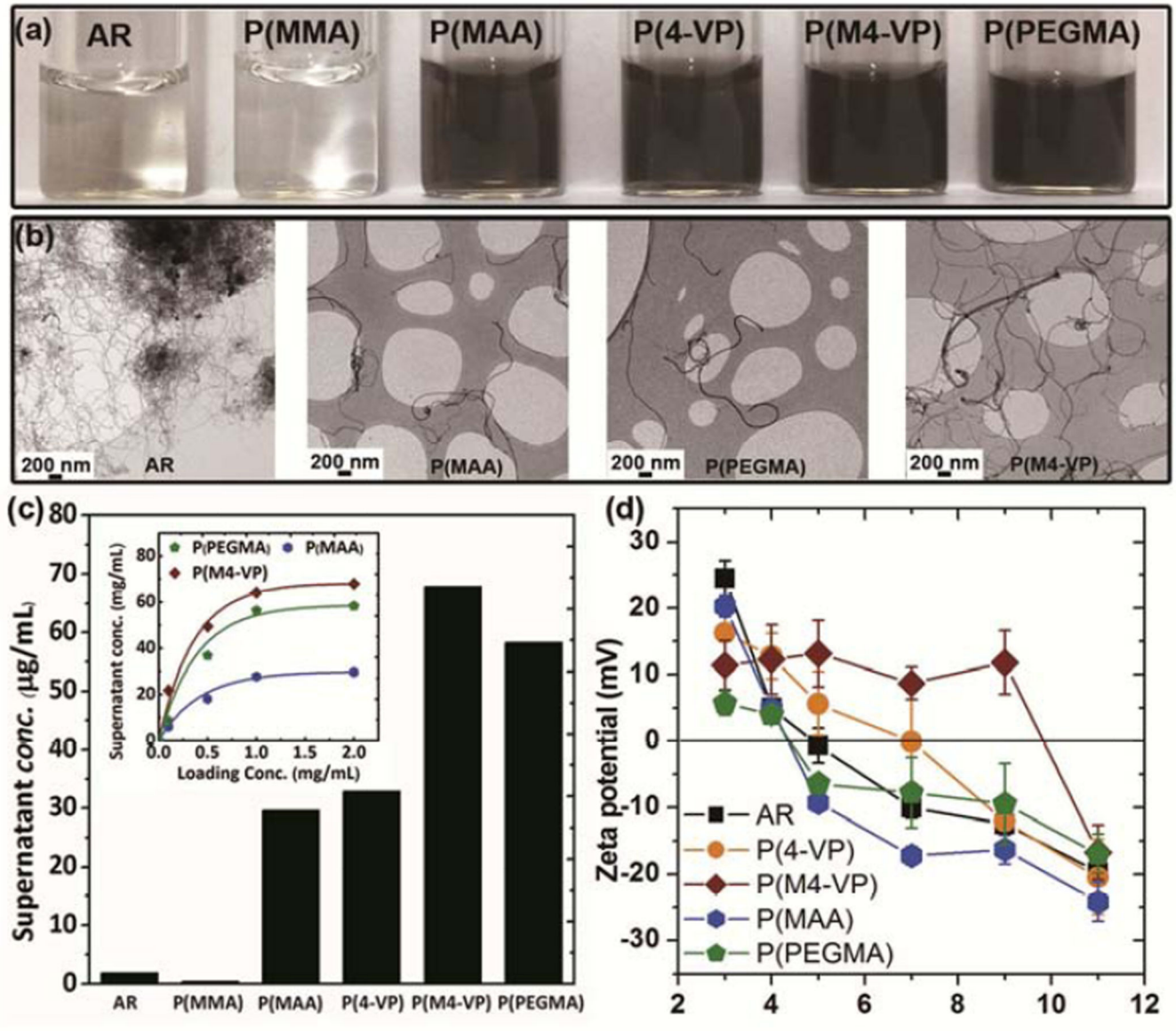

Figure 2.

(a) The water stability of MWNT samples is illustrated by photos showing the supernatants obtained by 15 minutes of bath sonication of MWNT-water mixtures with a starting concentration of 100 μg/mL followed by centrifugation (10, 000 g, 15 minutes); (b) low resolution BF-TEM images showing the isolated nature of grafted MWNTs as compared to AR-MWNT; (c) the supernatant concentrations of various grafted MWNTs were quantitatively determined by UV absorbance with a loading concentration of 2 mg/mL; inset are the supernatant concentrations of various grafted MWNTs in HPLC water with various initial loading concentrations, quantified by UV absorbance and (d) MWNT zeta-potential curves as a function of pH.

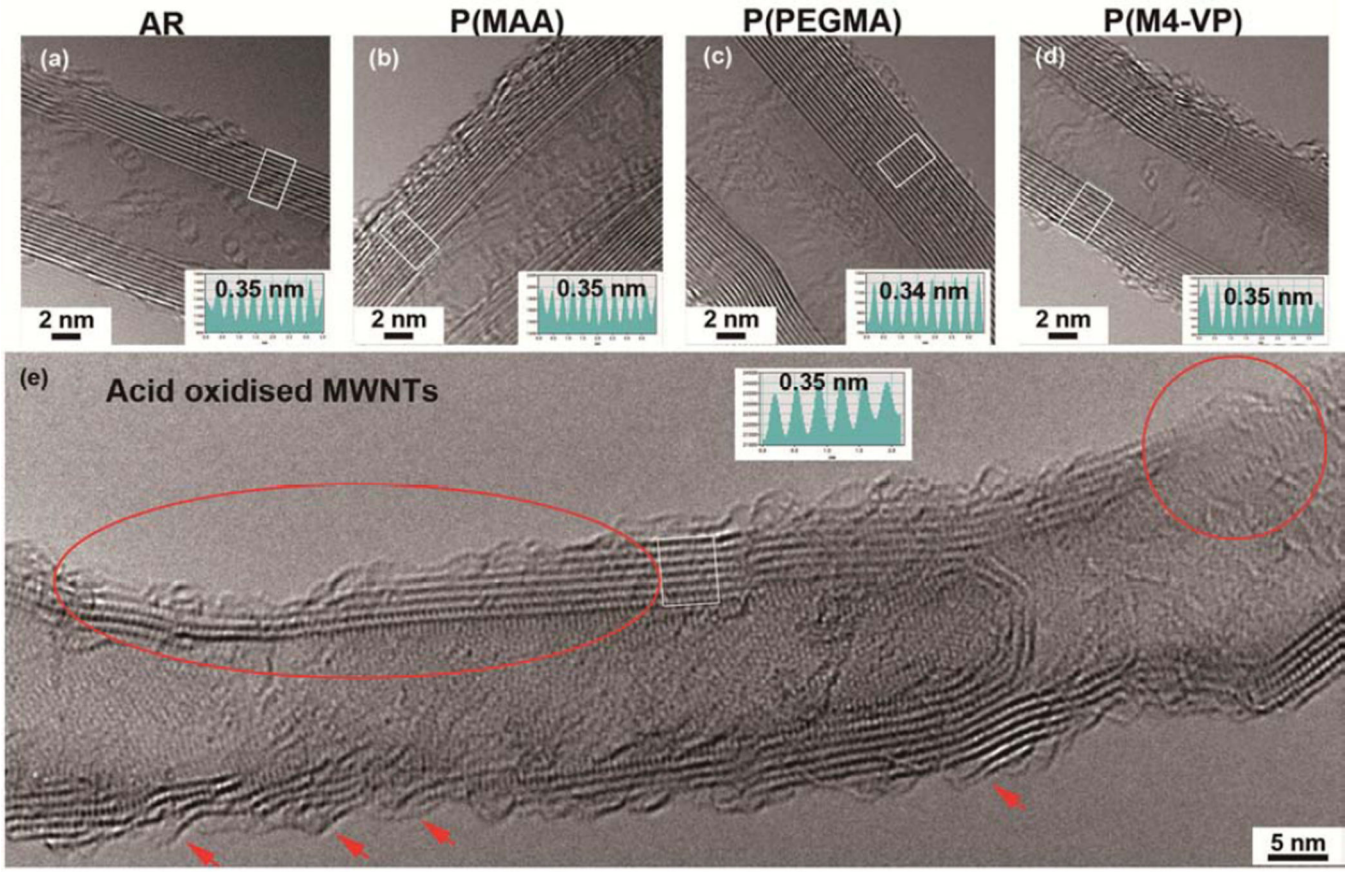

Figure 3.

HRTEM images and inserted intensity profiles taken from boxed areas to show the morphology and crystallinity of an (a) AR-MWNT, (b) P(PMAA)-MWNT, (c) P(PEGMA)-MWNT, (d) P(M4-VP)-MWNT and (e) acid oxidised MWNT. The characteristic features of the delamination, etching and pitting to the MWNT framework caused by acid oxidation process are marked.

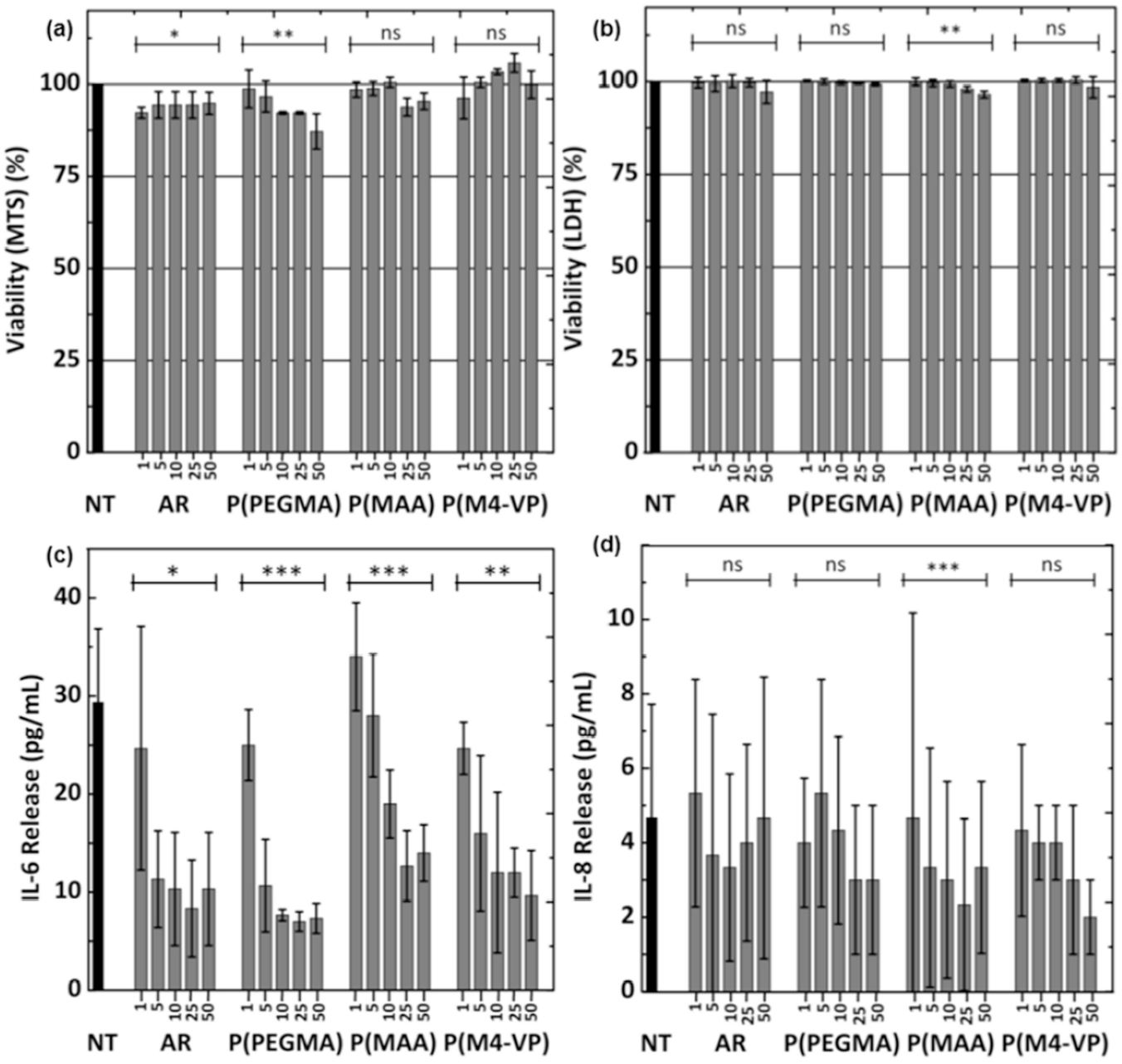

Figure 4.

Cytotoxicity (MTS assay (a), LDH assay (b)) and release of IL-6 (c) and IL-8 (d) induced by MWNTs on TT1 cells, following a 24 hours exposure at increasing concentrations up to 50 μg/mL. Error bars are mean ± SD (n = 3). *, $p < 0.05$; **, $p < 0.005$.

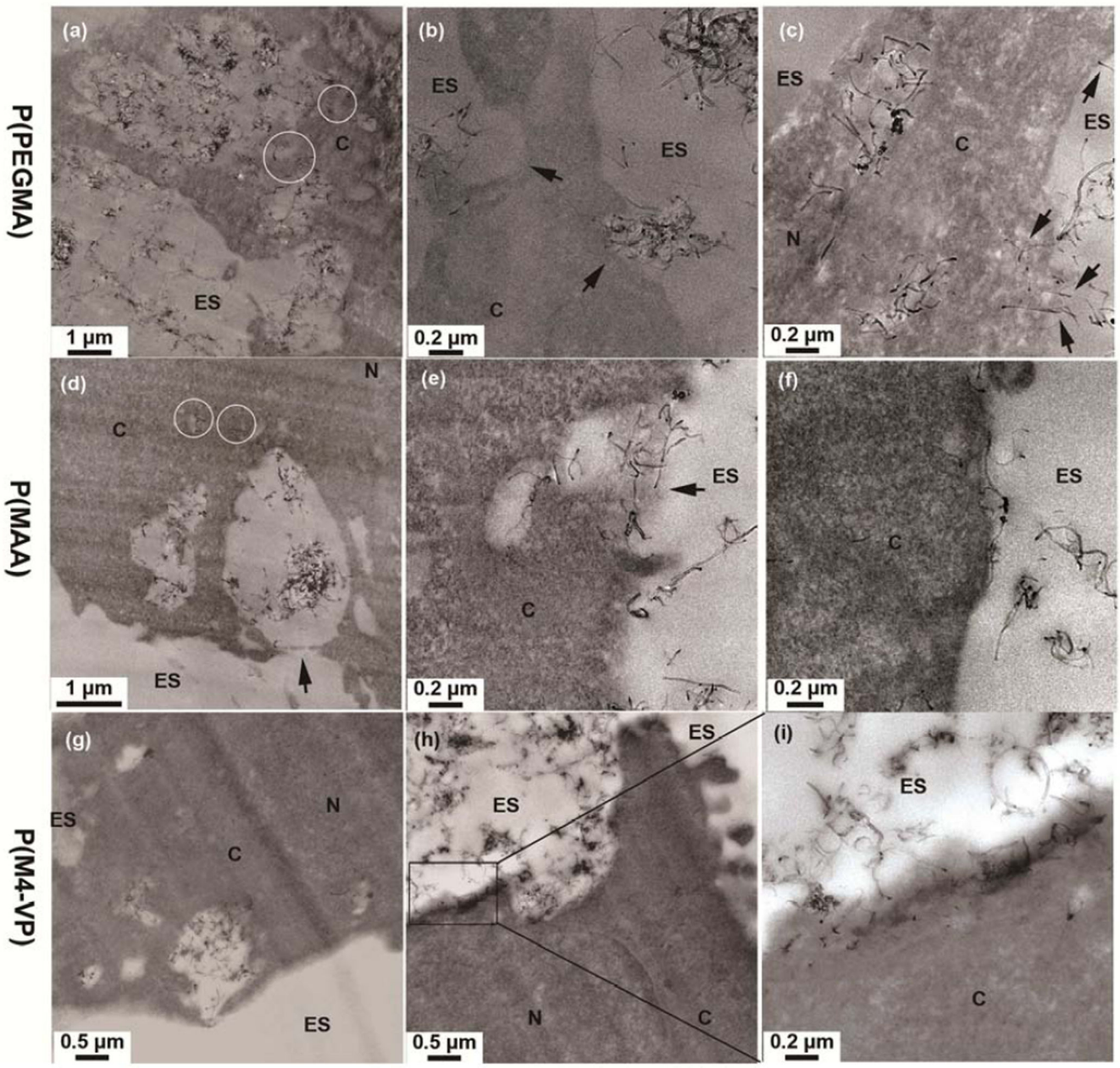

Figure 5.

TEM images showing the cellular distribution and interaction of (a–c) P(PEGMA)-MWNTs, (d–f) P(PMAA)-MWNTs and (g–i) P(M4-VP)-MWNTs with TT1 epithelial cells after 24 hours exposure. Individual MWNTs are indicated by circles. Figure 5i is a higher resolution TEM image of boxed area in Figure 5 h. ES= extracellular space; C=cytoplasm; N=nucleus.

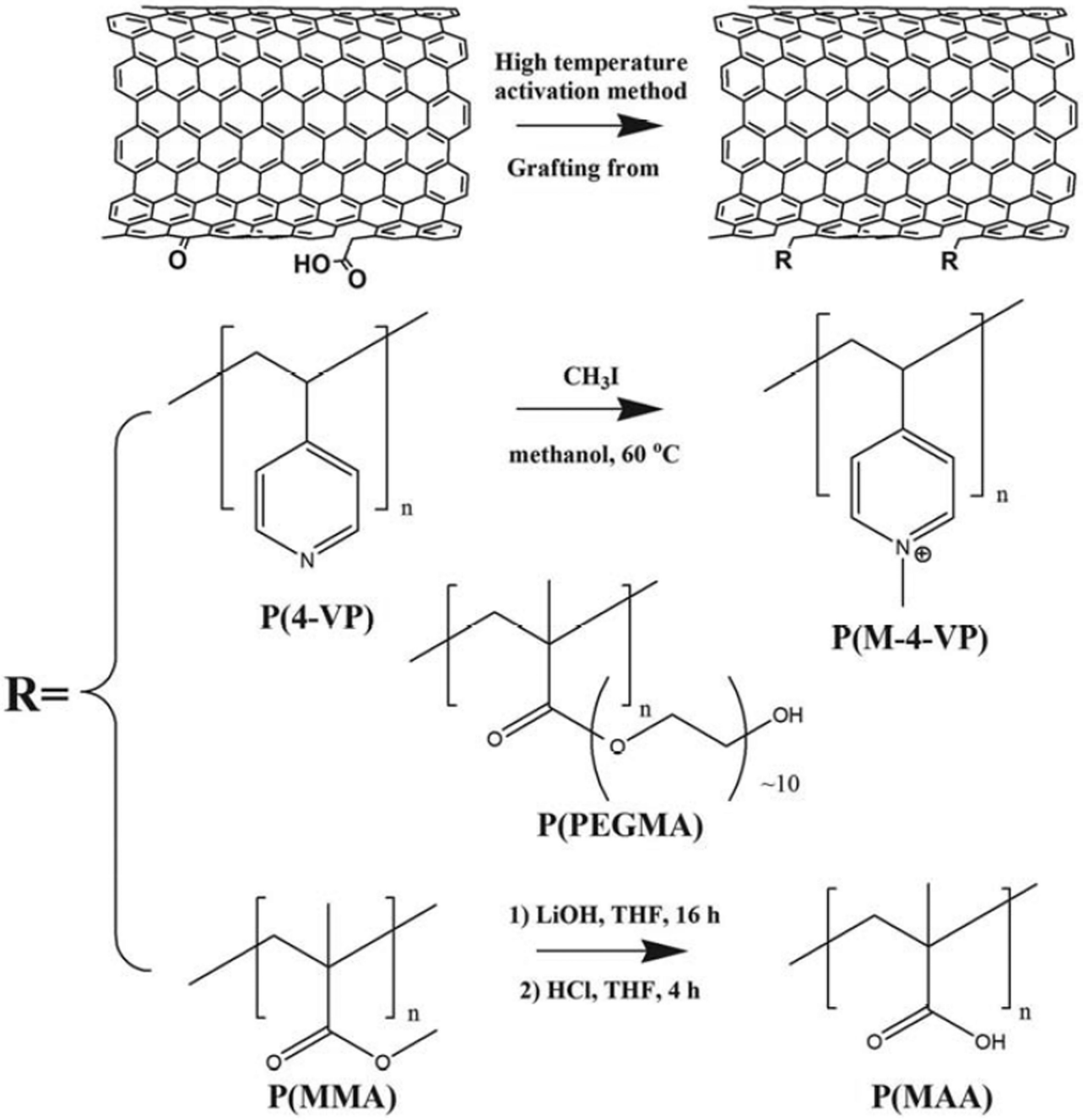

Scheme 1.

Reaction scheme for the thermochemical ‘grafting from’ MWNTs with various functional reactants. Refer to Table 1 for further details about the organic reactants used.

Table 1

Grafting ratios in weight loss, wt% (weight percentage of grafted oligomers in total grafted sample weight), grafting concentration (moles of monomer per gram of MWNTs) of MWNTs samples and estimated degree of polymerisation of monomers (repeating monomeric unit), calculated based on TGA profiles (Figure 1). Details of the grafting ratio calculations are described in the ESI Figure 1S–2S

Sample Code	Grafted Compound (chemical name)	M_w	Grafting Ratio (wt%)	Grafting Concentration (μmol/g)	Repeating Monomeric Unit
P(MMA)-MWNT	Methyl methacrylate	100.1	3.9	405	5
P(MAA)-MWNT	Methacrylic acid	86.1	3.4	409	5
P(4-VP)-MWNT	4-Vinylpyridine	105.1	4.1	407	5
P(M4-VP)-MWNT	N-methyl 4-vinylpyridine iodide	247.1	8.7	386	5
P(PEGMA)-MWNT	Poly (ethyleneglycol) methacrylate	528.9	18.3	423	5
IDD-MWNT	1-Iodododecane	169.3	1.4	84	1

Table 2

Maximum supernatant concentration (with loading concentration 2 mg/mL), zeta-potential in pH 7 HPLC water, isoelectric point (IEP) and D / G ratio of AR and grafted MWNTs. (The Raman spectra are presented in ESI Figure 3S.)

Sample Code	Maximum supernatant concentration in water (μg/mL)	Zeta-potential (mV) in pH 7 HPLC water	IEP	D/G ratio
AR-MWNT	1.9	−10.02 ± 1.59	5.0	1.09 ± 0.03
P(MMA)-MWNT	0.5	N/A	N/A	1.07 ± 0.08
P(MAA)-MWNT	29.6	−17.2 ± 1.3	4.3	1.03 ± 0.07
P(4-VP)-MWNT	32.9	−0.1 ± 6.4	7.0	1.05 ± 0.02
P(M4-VP)-MWNT	67.8	8.7 ± 2.4	9.8	1.04 ± 0.03
P(PEGMA)-MWNT	58.3	−7.8 ± 5.3	4.6	1.13± 0.09